

**Graphene-based membranes**

Journal:	<i>Chemical Society Reviews</i>
Manuscript ID:	CS-SYN-11-2014-000423.R2
Article Type:	Tutorial Review
Date Submitted by the Author:	01-May-2015
Complete List of Authors:	Liu, Gongping; Nanjing Tech University, State Key Laboratory of Materials-Oriented Chemical Engineering Jin, Wanqin; Nanjing University of technology, College of chemistry and Chemical Engineering Xu, Nanping; Nanjing Tech University, State Key Laboratory of Materials-Oriented Chemical Engineering

TUTORIAL REVIEW

Graphene-based Membranes

Cite this: DOI: 10.1039/x0xx00000x

Gongping Liu, Wanqin Jin* and Nanping Xu

Received 00th XXXX 2015,
Accepted 00th XXXX 2015

DOI: 10.1039/x0xx00000x

www.rsc.org/csr

Graphene is a well-known two-dimensional material that exhibits preeminent electrical, mechanical and thermal properties owing to its unique one-atom-thick structure. Graphene and its derivatives (e.g., graphene oxide) become emerging nano-building blocks for separation membranes featuring distinct laminar structure and tunable physicochemical properties. Extraordinary molecular separation properties for purifying water and gases have been demonstrated by graphene-based membranes, which attract a huge surge of interest during last a few years. This tutorial review aims to present latest groundbreaking advances in both theoretical and experimental chemical science and engineering of graphene-based membranes, including their design, fabrication and application. Special attention will be given to the progresses of processing graphene and its derivatives into separation membranes with three distinct forms: porous graphene layer, assembled graphene laminates and graphene-based composites. Meanwhile, critical views on separation mechanism within graphene-based membranes will be provided based on discussing the effect of inter-layer nanochannels, defects/pores and functional groups on molecular transport. Furthermore, the separation performance of graphene-based membranes applied for pressure filtration, pervaporation and gas separation will be summarized. This article is expected to provide a compact source of relevant and timely information and will be of great interests to all chemists, physicists, materials scientists, engineers and students entering or already working in the field of graphene-based membranes and functional films.

Key learning points

- (1) Overview of emerging graphene-based membranes and their significant implications in molecular separation
- (2) Theoretical and experimental chemical science and engineering of graphene-based membranes
- (3) Strategies of exploring graphene and its derivatives to construct membranes with well-defined nanostructures and ultra-fast and highly-selective permeation properties
- (4) Transport properties and separation mechanism in porous layer, laminates and composites derived from graphene-based materials
- (5) Application paradigms of graphene-based membranes for purifying water and gases

1 Introduction

In the last two decades, membrane separation has become an advanced technology for solving the enormous challenges that the mankind faces such as resources and environmental problems. Compared with conventional separation methods, membrane separation is an energy-efficient and environmentally benign technology occupied less space and operated in a continuous mode¹. An ideal membrane should provide higher permeate flux, higher selectivity and improved stability through controlled pore size and shapes. Meanwhile, the reduction of membrane thickness is essential to maximize permeability, and to achieve higher throughput and increase membrane performance.

Polymeric and inorganic membranes have dominated the research and development attention in the past, but most of

them are constrained by a trade-off between permeability and selectivity or high fabrication cost. Recently, materials with well-defined nanostructures such as zeolites, metal organic frameworks and carbon-based materials show great potential in membrane development owing to their excellent separation performance and reliable processing strategies. Among them, carbon nanotubes (CNTs) were regarded as one of the most promising candidates for the breakthrough of conventional membranes because of the unique one-dimensional nanochannel for ultra-fast molecular transport, as well as superb mechanical strength. However, CNT-based membranes are basically limited to theoretical studies because of several technical challenges such as relatively high cost of CNTs, complex process of obtaining high density of vertically-aligned CNTs, and difficulties for achieving large-scale production. Besides of the one-dimensional CNTs, recent rise of synthesis

and processing of two-dimensional (2D) graphene and its derivatives offers an exciting opportunity to develop a new class of membranes with extraordinary separation properties^{2,3}. Here, we refer graphene-based materials to graphene, graphene oxide and chemically-converted graphene. The only one-atom thickness and nearly frictionless surface enables them to form membranes that minimize transport resistance and maximize permeate flux. In addition, the outstanding mechanical strength and chemical stability, together with cost-effective production, allows graphene-based membranes for practical application⁴.

The perfect single-layer graphene sheet is impermeable to gases as small as helium⁵, due to the fact that the electron density of its aromatic rings is substantial enough to repel atoms and molecules trying to pass through these rings⁶. Therefore, initial theoretical studies focused on drilling holes in graphene sheet to make porous graphene membranes for selective passage of water⁷, ions⁸ and gases⁹. Although exciting separation performance is predicted, there remains a great challenge to perforate selective pores in large-area despite a few attempts being made recently^{10, 11}. Alternatively, graphene, especially graphene oxide (GO) nanosheets can be assembled into laminar structures via filtration or coating approaches, providing fast and selective 2D nano-channels for transporting small molecules. The pioneering work of Geim et al. found that submicrometer-thick laminates formed from GO can be completely impermeable to liquids, vapors and gases, but allow unimpeded permeation of water¹². From then on, the assembled GO membranes have been reported for applications in water purification¹³⁻¹⁵ and solvent dehydration^{16, 17}. Meanwhile, graphene-based laminates can also exhibit gas separation characteristics if their stacking structures are carefully controlled^{18, 19}. Apart from the all-graphene membranes, graphene-based composites^{20, 21}, which generally combined graphene or GO nanosheets with polymers or inorganics, have gained ground as a means of improving selective-permeation and/or anti-fouling properties of the pristine membranes. Graphene-based membranes constructed by different approaches possessed distinct microstructures and transport pathways, enabling them to be applied for various membrane processes such as pressure filtration (e.g., ultrafiltration¹⁴, nanofiltration^{13, 22}, reverse osmosis²³, forward osmosis¹⁵), pervaporation^{16, 21, 24, 25} and gas separation¹⁸⁻²⁰.

Since the 2010 Nobel Prize for “groundbreaking experiments regarding the two-dimensional material graphene”, there are exponentially growing papers focusing on the significant interest of graphene-based separation membranes. A recent feature article focused on summarizing physicochemical properties of GO membranes and their applications in pressure-driven separation²⁶. Another two review papers on graphene-based materials for desalination were appeared very recently^{27, 28}. The vast amount of literature demonstrates that the important contemporary topic “graphene-based membranes” has now reached the stage where a timely overview is necessary to cover latest progress, emerging trends and opening opportunities. This tutorial review is therefore intended to serve this purpose. It presents advances in both theoretical and experimental chemical science and engineering of graphene-based membranes, including principle, design, fabrication, characterization and application. Special attention will be given to strategies of using graphene-based materials to develop membranes with controlled microstructures. Meanwhile, we will provide critical views on understanding transport behavior and separation mechanism through porous graphene layer, graphene laminates and graphene composites. This contribution

will also look into future prospective of emerging graphene-based membranes for implementation in water resources, energy and environment fields.

2. Physicochemical properties and fabrication approaches

2.1 Properties and synthesis of graphene-based materials

Prior to talk about graphene-based membranes, the intrinsic properties and synthesis of graphene-based materials will be briefly introduced since they strongly determine the membrane preparation, microstructures and separation performance. Graphene is a single atom thick sheet of sp² hybridized carbon atoms arranged in honeycomb lattice, which is regarded as the thinnest 2D material⁶. Since its successful isolation in 2004, significant interest has been focused on graphene in various fields such as fundamental physics, chemistry, materials science and device applications⁴. In particular, the unique one-atomic thickness and two-dimensional structure, in addition with high mechanical strength and chemical inertness of graphene open up many potential opportunities for materials applications, including separation membranes. As one of the most important derivatives of graphene, GO exhibits similar properties as graphene, except lots of oxygen-containing functional groups, for instance, epoxy, hydroxyl, carbonyl and carboxyl groups, on edges and basal planes of the sheet²⁹. These oxygen functional groups facilitate readily tuning the physicochemical properties of GO sheet as well as its derived membranes. On the one hand, the hydrophilic groups enable stable dispersions of GO sheets in aqueous media, which provide a facile processing and stacking of these sheets³⁰. On the other hand, the functional groups provide reactive handles for various modifications of GO, so as to readily control the microstructures and chemical properties of GO membranes, as well as develop GO-based hybrid membranes. Besides, molecular transport within GO-based membranes is particularly benefited from those oxygen atoms bonded to carbon atoms: 1) these groups could form hydrogen bonding with water⁷ or gases such as CO₂¹⁸, and electrostatic interaction with ionic components²², enhancing preferential permeation properties of GO membranes; 2) the oxidized regions of graphene play a role of spacers that keep graphene planes about 0.7 to 1.0 nm apart in GO laminates, and the pristine regions create almost frictionless 2D nanochannels for transporting small molecules across GO laminates¹².

In general, methods for producing graphene can be classified into five main classes³¹: 1) mechanical exfoliation of a single sheet of graphene from bulk graphite manually using Scotch tape or automatically using sonification; 2) crystal growth of graphene films; 3) chemical vapor deposition (CVD) of graphene monolayers; 4) longitudinal cutting of CNTs and 5) reduction of graphene derivatives such as GO. Despite Scotch-tape and CVD techniques have been employed to produce high-quality graphene monolayer, the ultrasonic cleavage of graphite and reduction of graphene derivatives allow scalable production of graphene layers⁴. Generally, GO is synthesized based on Brodie, Staudenmaier and Hummers methods³¹, involving oxidation of graphite to various levels. The extent of graphite oxidation, as quantified by carbon/oxygen ratio, is dependent upon the synthetic technique as well as the length of reaction. Readers are suggested to refer a comprehensive review on synthesis, structure and chemical reactivity of GO²⁹. The favorable physicochemical properties and synthesis approaches

of graphene-based materials enable them to be used as versatile 2D building blocks to fabricate molecular-selective membranes. As given in Figure 1, there are three main types of graphene-based membranes according to the microstructures: 1) porous graphene layer, 2) assembled graphene laminates and 3)

graphene-based composite. They are discussed in the following section one by one.

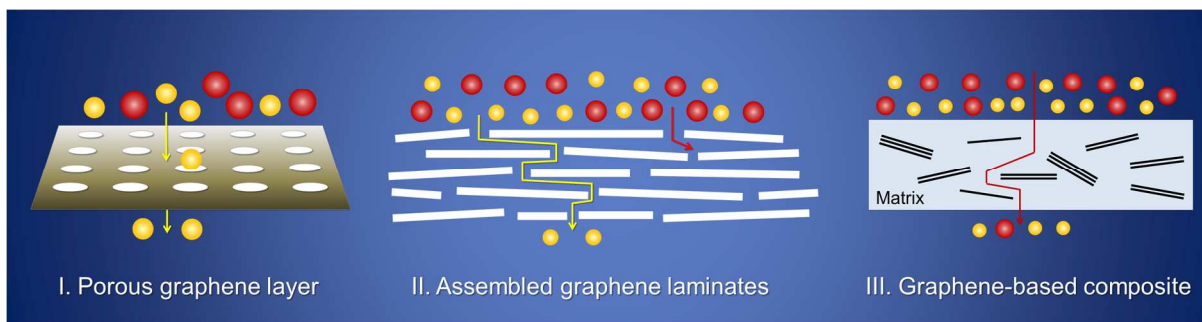


Fig. 1 Main types of graphene-based membranes: Type I. porous graphene layer; Type II. assembled graphene laminates; Type III. graphene-based composite.

2.2 Porous graphene layer

One of the most exciting features of graphene sheet is its one-atom thickness, therefore being the ultimate membrane, because the membrane permeance is generally inversely proportional to the membrane thickness¹. At first, Bunch et al.⁵ tested the permeance of several gases through a micro-chamber capped with a graphene sheet mechanically exfoliated from Kish graphite by the Scotch tape technique (Figure 2a-b). The monolayer graphene membrane was demonstrated to be impermeable to gases as small as helium. This is due to the fact that graphene's π -orbitals form a dense, delocalized cloud that blocks the gap within its aromatic rings. Berry's theoretical calculation⁶ further indicated that there is no gap in electron-density around the aromatic rings to allow molecules to pass, as shown in Figure 2c. If the radius of carbon of 0.11 nm is added, this geometric pore size of graphene would decrease from 0.246 to 0.064 nm, which is smaller than the diameter of small molecules like helium (0.28 nm) and hydrogen (0.314 nm). Moreover, the one-atom-thick graphene membrane can withstand pressure differences as high as 6 atm, resulting from its excellent mechanical property. This impermeable and robust graphene sheet motivated the theoretical and experimental studies on perforated graphene membrane as selective barrier for separation. Here, we refer this type of membrane as "porous graphene membranes".

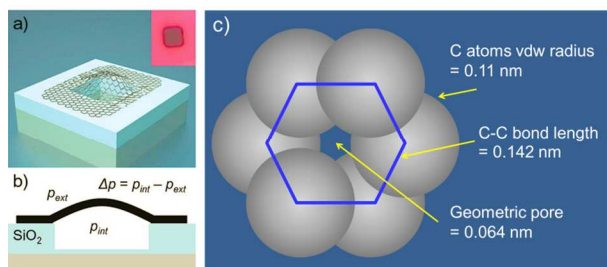


Fig. 2 (a) Schematic of a graphene sealed microchamber. (Inset) optical image of a single atomic layer graphene drumhead on 440 nm of SiO₂. The dimensions of the microchamber are 4.75 μm \times 4.75 μm \times 380 nm; (b) Side view schematic of the graphene sealed microchamber. Reproduced with permission from ref. 5. Copyright 2008, American Chemical Society; (c) theoretical calculation of geometric pore on graphene, vdw: Van der Waals. Reproduced with permission from ref. 6. Copyright 2013, Elsevier.

Sint et al.⁸ used molecular dynamics simulations to study diffusion of ions (Li⁺, Na⁺, K⁺, Cl⁻, and Br⁻) through graphene monolayers with functionalized nanopores of 5 Å diameter, and observed that pores terminated by negatively charged F–N highly favor the passage of cations, while H-terminated nanopores with positive charge facilitate the passing of anions. Their study demonstrated the viability of nanoporous graphene monolayer as ion separation membranes applied for desalination and energy storage. Similarly by virtue of molecular simulation, Cohen-Tanugi and Grossman⁷ investigated water desalination across nanoporous single-layer graphene with the variation of pore size and functional (Figure 3). They found that hydrogen-terminated nanopores showed better water selectivity while graphene pores functionalized by hydroxyl groups double the water flux, which was attributed to their hydrophilic character and ability to substitute for water molecules in the hydration shell of the ions. The calculated water permeability of 66 L/cm²/day/MPa through the nanoporous graphene is 2-3 orders of magnitude higher than conventional reverse osmosis membranes with similar salt rejection of 99 % (Figure 3). These values revealed a great potential to utilize functionalized nanoporous graphene sheets as a high-permeability desalination membrane. The feasibility of porous graphene sheets for gas separation was simulated by Jiang et al.⁹. According to their computed diffusion barriers, H₂/CH₄ selectivity was as high as the order of 10⁸ and 10²³ through the one-atom-thin graphene sheet, respectively for the designed N-functionalized (3.0 Å) and the all-H pores (2.5 Å).

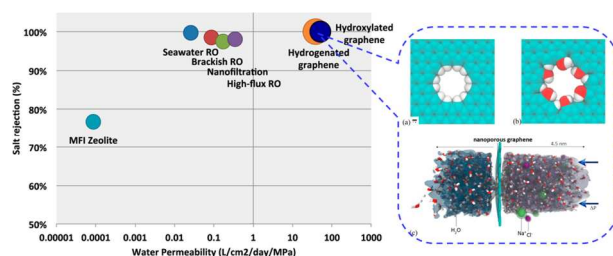


Fig. 3 (Left) Performance chart for functionalized nanoporous graphene versus existing technologies. (Right) Hydrogenated (a) and hydroxylated (b) graphene pores, and (c) side view of the computational system. Reproduced with permission from ref. 7. Copyright 2012, American Chemical Society.

Overall, simulation works on the molecular sieving property of porous single-layer graphene predicated that imparting controlled nanopores to graphene sheet can render graphene an ultimate thin membrane for liquid and gas purification. Such proposed vision strongly depends on the techniques of monolayer fabrication and “drill holes” in the graphene sheet. Single graphene layer for developing porous graphene membrane is usually produced via Scotch tape method or CVD approach. It is necessary to carefully control the CVD process; otherwise intrinsic pores are possible found in the obtained graphene sheet due to grain-boundaries and point defects. Recent experimental investigations, using oxidative etching³², electron/ion bombardment¹⁰ or bottom-up synthesis⁴ to create pores in graphene, open the door to utilize variable-sized graphene nanopores to achieve molecular separation performance.

A notable step towards the realization of macroscopic, size-selective porous graphene membranes was made by Bunch and co-workers³². Ultraviolet-induced oxidative etching technique was employed to create Angstrom scale pores in 5- μm -diameter bilayer graphene sheet produced by the Scotch tape method. Followed by their previous work⁵, a pressurized blister test and mechanical signals are used to measure gases transport through the porous graphene membranes. The obtained separation performance partially agreed with simulation results based on effusion through a small number of angstrom-sized pores, which will be discussed in Section 3.2.3. While the several orders of magnitude lower in permeate rate and selectivity were attributed to two possible reasons³²: 1) the etched pores with an overall higher energy barrier for gases than in simulation and 2) different chemical pore termination. Another recent experiment study demonstrated that single-layer porous graphene can be used as a desalination membrane²³. Nano-sized (0.5-1 nm) pores are created in a graphene monolayer by employing oxygen plasma etching process to tune the pore size. Nearly 100% salt rejection and 10^6 g/m²/s water flux were obtained using pressure difference as a driving force. However, with practical osmotic pressure as a driving force, the water flux did not exceed 250 L/m²/h/bar that is much lower than the simulated result. The authors attributed it to ions binding to the nanopore termination groups, which block the water flux.

It was also noticed that the above-mentioned methods limit to create a small density of pores in micrometer-sized graphene layer. An interesting attempt to perforate large-area and sub-nanometer pores in single-layer graphene membrane was accomplished by Karnik and co-workers¹¹. Isolated and reactive defects were first introduced into the graphene lattice through ion bombardment and subsequently enlarged by oxidative etching. They obtained permeable pores with diameters of 0.40 ± 0.24 nm and densities exceeding 10^{12} cm⁻², while kept structural integrity of the graphene. Ionic transport through these pores was highly selective and tunable by simply controlling the etch time, highlighting the potential application in water purification. Very recently, Celebi et al.¹⁰ developed an optimized CVD growth followed by focused ion beam approach to realize physical perforation of bilayer graphene having narrowly distributed pore sizes ranging from <10 nm to 1 μm and large number of pores ($\sim 10^3$ to 10^6 per membrane), as shown in Figure 4. In their practical separation experiment carried on the atomically thin porous graphene, orders-of-magnitude enhancements are observed for gases, water and water vapor permeance, compared with the state-of-the-art membranes.

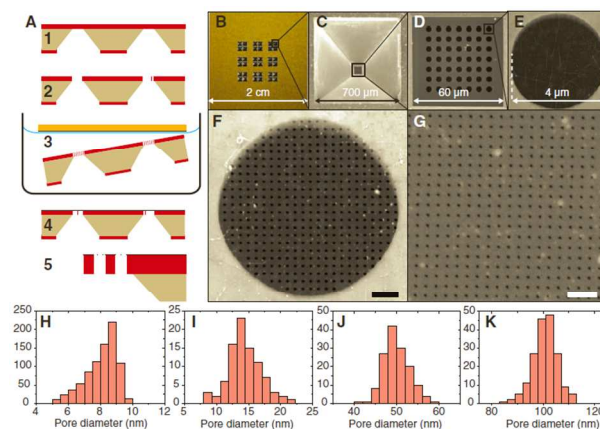


Fig. 4 Membrane fabrication and diameter distribution. (A) Schematic of the porous graphene fabrication process. Step 1: freestanding SiN_x membrane formation (by means of KOH etching). Step 2: microscale pore formation through the SiN_x membrane (by means of photolithography and reactive ion etching). Step 3: graphene transfer. Step 4: graphene surface cleanup. Step 5: physical perforation of graphene by means of Ga- and He-based focused ion beam (FIB) drilling. (B) Photograph (bottom view) of a full membrane structure. (C) Bottom view SEM image of the SiN_x membrane. (D to G) Top view SEM images of (D) porous freestanding SiN_x window before graphene transfer, (E) freestanding graphene transferred on one of the 4-mm-wide SiN_x open pores, (F) 50-nm-wide apertures FIB-drilled on the freestanding graphene (Ga FIB) (scale bar, 500 nm), and (G) 7.6-nm-wide apertures perforated in the similar way (He FIB) (scale bar, 100 nm). (H to K) Aperture size distributions of the (H) 7.6-nm-, (I) 16-nm-, (J) 50-nm-, and (K) 100-nm perforated graphene membranes. Reproduced with permission from ref. 10. Copyright 2014, the American Association for the Advancement of Science.

2.3 Assembled graphene laminates

Many theoretical calculations and a few experimental studies indicated that porous monolayer graphene membranes showed great potential in water purification and gas separation. Nevertheless, precise, large-area and high-density perforation, as well as practical modularization of porous graphene layer remain technical challenges. Alternatively, graphene derivatives can be readily assembled into well-ordered macroscopic structures. For instance, single-atom-thick with lateral dimensions as high as tens of makes GO highly stackable for laminates³¹. In addition, GO nanosheets can be mass-produced via chemical oxidation and ultrasonic exfoliation of graphite, thus significantly reducing the membrane cost²⁹. Particularly, the oxygen-containing groups on GO provide active sites for further functionalization to enhance properties such as charges and specific interactions with ions and molecules. These features opened up a more practical route of facile and large-scale production of graphene-based membranes^{3, 33}.

2.3.1 Preparation methods of assembled laminates

Free-standing GO papers were fabricated by flow-directed (i.e., filtration) assembly of GO sheets³⁰, resulting in tightly packed interlocking sheets that subtly undulate along the paper surface. The layered structure with sub-nanosized inter-layer spacing, and the excellent macroscopic flexibility and stiffness, promise practical utilization of such GO laminates for molecular separation. The slowly flowing water in the confined galleries, together with the electrostatic and van der Waals attractive

forces between the very large aspect ratio compliant sheets of GO, are largely responsible for their sequential deposition into the laminar structure. Driving force of the filtration plays a critical role in determining the nanostructures of GO stacks. As shown in Figure 5a, the nanosheets orientation of GO membranes assembled by pressure-assisted, vacuum-assisted and evaporation-assisted methods, were found to be highly ordered, random and highly random with some loop pattern formations, respectively³⁴. XRD results indicated that the *d*-spacing of these membranes varied from 8.3 Å to 11.5 Å. In addition, considering delicate size selection and layer thickness reduction, centrifugation and dilution of GO dispersions were found to be important for preparing high-quality GO membranes¹⁹.

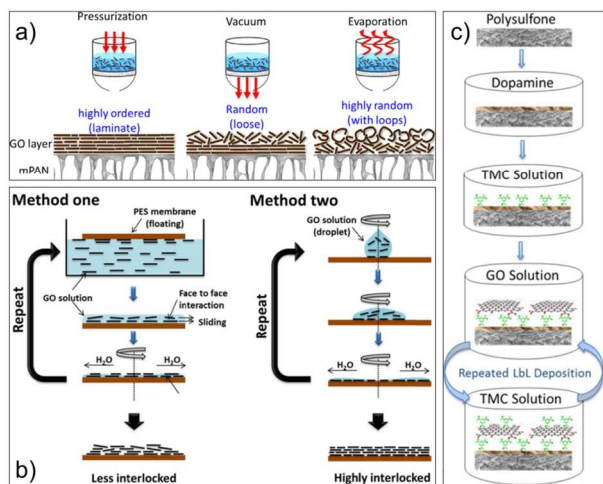


Fig. 5 Schematic of assembled GO laminates prepared by different methods: (a) pressure-assisted self-assembly, vacuum-assisted self-assembly, and evaporation-assisted self-assembly. Reproduced with permission from ref. 34. Copyright 2015, Elsevier; (b) spinning coating methods. Reproduced with permission from ref. 18. Copyright 2013, the American Association for the Advancement of Science; and (c) layer-by-layer method. Reproduced with permission from ref. 22. Copyright 2013, American Chemical Society.

Besides the filtration method, various coating approaches have been proposed to assemble GO sheet into laminar membranes, including spray-coating¹², spin-coating¹⁸, drop-casting³⁵ and dip-coating³⁶. Kim et al.¹⁸ compared the nanostructures of few-layered GO membranes via two coating methods: 1) contacting the substrate surface to the air-liquid interface of a GO solution, followed by spin-coating; 2) spin-casting of a GO solution on the substrate surface (Figure 5b). It was indicated that the stacking of GO nanosheets is governed by intrinsic repulsive edge-to-edge GO sheet interaction and face-to-face attractive capillary forces created by the spin-coating. In the method 1, the initial electrostatic repulsion between the GO edges leads to a relatively heterogeneous GO deposition, in which the GO stacking structure resembles islands. In contrast, in method 2, the GO solution-membrane contact occurs only during spin-casting, leads to a highly interlocked laminates. The dense stacking occurs because the capillary interactions between the faces of GO sheets overcome the electrostatic forces between the GO edges.

Laminar GO membranes can also be synthesized via layer-by-layer assembly of GO nanosheets. This approach is ideal for introducing an interlayer stabilizing force via covalent bonding or electrostatic interaction, or both effects during layer deposition. The thickness of GO membrane can be easily

adjusted by varying the number of layer-by-layer deposition cycles. Hu and Mi²² enabled GO nanosheets as water separation membranes via this method, which were cross-linked by 1,3,5-benzenetricarbonyl trichloride (TMC), as shown in Figure 5c. The spacing between GO layers sandwiched by TMC molecules (0.7 nm) is estimated to be around 1 nm. The cross-linking process not only regulated the charges, functionality and spacing of the GO nanosheets, but also provided the stacked GO nanosheets with necessary stability to overcome their inherent dispensability in water environment.

Generally, with the desire of practical application, it is indispensable to develop GO composite membranes that consist of thin GO separation layer and porous support layer. Compared with flat substrate for most GO membranes, hollow fibers exhibit many advantages, such as high packing density, cost-effectiveness and self-supporting structure. We have constructed an integrated and continuous GO membrane on a hollow fiber substrate by vacuum suction method. As shown in Figure 6, GO nanosheets can be easily stacked on the curved surface of the hollow fiber despite of its high curvature and elongated shape¹⁶. The hollow fiber GO membrane exhibited excellent selective water permeation when treating aqueous dimethyl carbonate solution. Moreover, the interfacial adhesion between GO layer and supporting layer is another key for practical use of GO composite membranes, although little attention has been paid to this issue. A facile silane-graft modification approach proposed by our group was demonstrated to be an efficient way to improve the quality of GO film formation on porous substrate. More importantly, the interfacial adhesive force of GO composite membrane was highly enhanced from 12.07 mN to 38.78 mN³⁶.

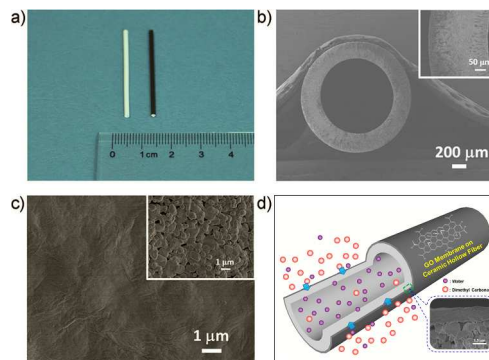


Fig. 6 (a) Photographs of the blank hollow fiber (white) and the GO membrane (black); SEM images of (b) a ceramic hollow fiber (insert: an enlarged cross-section of the ceramic hollow fiber) and (c) surface and of the blank hollow fiber (inset) and the GO membrane; (d) schematic of hollow fiber GO membranes for selective water permeation of aqueous dimethyl carbonate solution inset: SEM image of cross-section of the hollow fiber GO membrane). Reproduced with permission from ref. 17. Copyright 2014, John Wiley and Sons.

2.3.2 Nanostructures controlling of assembled laminates

Initially, Geim and co-workers¹² investigated the permeation of gases and liquids through free-standing submicrometer-thick (0.1–10 μm) GO membranes fabricated by spray- or spin-coating of GO water suspension (Figure 7a–b). Permeation measurements (Figure 7c) suggested that the GO membranes were completely impermeable to liquids and gases, including helium, which is in accordance with the impermeability of graphene sheet demonstrated by Bunch et al.⁵ (Figure 2a–b). However, a huge weight loss was unexpectedly observed in the water-filled container, with the

evaporation rate of water as same as in the absence of the GO membrane. The unimpeded permeation of water was more than 10^{10} times faster than He, as shown in Figure 7d. When the container was filled with mixtures of water and other gases and liquids, the permeation rate of water is also at least five orders of magnitude higher than that of others. They attributed the ultra-fast transport of water to a low-friction flow of monolayer of water through 2D capillaries formed by closely spaced graphene sheets. Diffusion of other molecules is blocked by reversible narrowing of the capillaries in low humidity and/or by their clogging with water. The transport mechanism will be further discussed in Section 3.1.

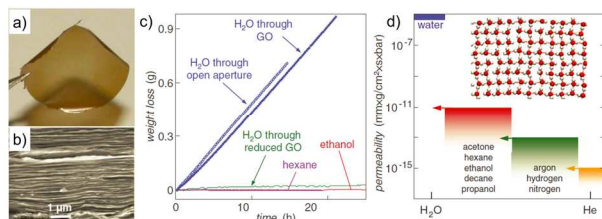


Fig. 7 He-leak-tight GO membranes: (a) Photo of a 1- μm -thick GO film peeled off of a Cu foil; and (b) Electron micrograph of the film's cross section; Permeation through GO: (c) weight loss for a container sealed with a GO film ($h \approx 1 \mu\text{m}$; aperture's area $\approx 1 \text{ cm}^2$). No loss was detected for ethanol, hexane, etc., but water evaporated from the container as freely as through an open aperture (blue curves). The measurements were carried out at room temperature in zero humidity; and (d) permeability of GO paper with respect to water and various small molecules (arrows indicate the upper limits set by our experiments). (Inset) Schematic representation of the structure of monolayer water inside a graphene capillary with $d = 7 \text{ \AA}$, as found in MD simulations. Reproduced with permission from ref. 12. Copyright 2012, the American Association for the Advancement of Science.

A large amount of subsequent studies on laminar GO membranes, however, revealed seemingly incompatible observations relevant to the above blocking permeation of liquids and gases except water. For examples, micrometer-thick GO laminates exhibited selective ion permeation if immersed in water³⁷, and few-nanometers-thin GO membranes could also allow fast-selective transport of water¹³ and gases^{18, 19}. It is due to the fact that the molecular sieving properties of GO membranes are strongly dependent on their nanostructures (e.g., inter-layer spacing, intrinsic defects) and functional groups.

Generally, GO sheets have two types of regions: functionalized (oxidized) and pristine (non-oxidized)¹². The former regions act as spacers that keep adjacent sheets apart and also help water to intercalate between GO sheets once in a hydrated state. The pristine regions provide a network of capillaries that allow nearly frictionless flow of correlated water, similar to the case of water transport through CNTs. In dry state, GO laminates are vacuum-tight with a typical inter-layer spacing (d) of $9 \pm 1 \text{ \AA}$. Taking into account d for reduced GO of 4 \AA , the empty space's width (pore size) can be estimated as $5 \pm 1 \text{ \AA}$, which allows one monolayer of moving water within the capillaries¹². When GO laminates soak in aqueous solution, the hydrophilic oxygen-containing groups can absorb a large number of water molecules. Thus the nanocapillaries open up and d would be enlarged to more than 13 \AA , providing larger pore size and 2D channels for transporting various small molecules³⁷. According to the Geim's report, the wetted micrometer-thick GO laminates prepared by vacuum filtration acted as molecular sieves that blocked all solutes larger than 9 \AA , meanwhile permeated smaller ions at rates thousands of times faster than what is expected for simple diffusion.

Similarly, Zhu and co-workers³⁵ found that sodium salts permeated quickly through freestanding GO membranes prepared via drop-casting. However, heavy-metal salts infiltrated much more slowly, and copper sulfate and organic contaminants (e.g. rhodamine B) are blocked entirely. Besides of the nanocapillaries within GO laminates, the chemical interactions between oxygen-containing groups of GO and metal ions were also demonstrated to be responsible for the selective ion permeation properties.

As the prominent characteristic of GO laminates, inter-layer spacing has been proved to play a significantly important role in molecular transport. It can be modulated by physical (e.g., stacking GO sheet with nanoscale wrinkles³⁸) or chemical approach (e.g., molecular intercalation²⁴ and thermal treatment³⁹). Due to the presence of some sp^3 hybridized carbon atoms and topological defects, chemically-converted graphene (CCG) is more susceptible to corrugation compared to pristine graphene (Figure 8a). Thus, stacking of these corrugated sheets will result in the formation of fuzzy nanochannels through the laminates that are permeable to liquids or gases (Figure 8b). Qiu et al.³⁸ revealed that the extent of corrugation of CCG sheets in water can be readily controlled by hydrothermal treatment, resulting in the filtrated wet CCG membranes with estimated size of nanochannels from 3 to 9 nm. The nanochannel network in the GO laminates, if well manipulated, is promising for pursuing efficient separation. Recently, Peng and co-workers¹⁴ used $\text{Cu}(\text{OH})_2$ nanostrands as sacrificial templates to prepare nanostrand-channelled GO membranes. $\text{Cu}(\text{OH})_2$ nanostrands of 2.5 nm in diameter and micrometers in length, with positive surface charges, tightly combined with GO sheets by electrostatic attraction (Figure 8c) when mixed with negatively charged GO. After the nanostrands were removed by an acid solution, a network of nanochannels with a narrow size distribution of 3-5 nm was formed. The water permeance ($695 \pm 20 \text{ L/m}^2/\text{h}/\text{bar}$) of such membranes is 1-2 orders of magnitude higher than that of commercial ultrafiltration membranes with similar rejection. In addition, the controlled removal of water trapped between the stacked GO layers is able to tailor the layer stacking orientation and the microstructure of GO membrane.

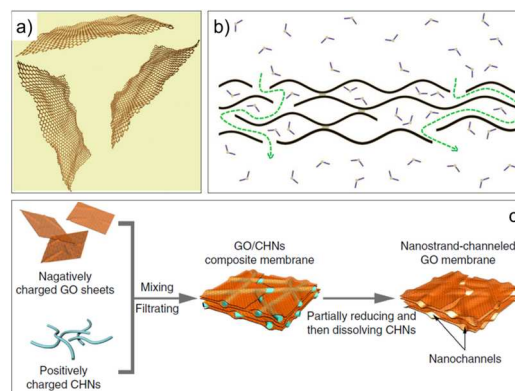


Fig. 8 (a) Schematic of graphene sheets suspended in a liquid showing how they could be corrugated; and (b) water molecules flowing through a corrugated CCG membrane. The dashed line indicates possible water flow paths. Reproduced from reference 38, Copyright RSC; (c) illustration of the fabrication process of nanostrand-channelled GO membrane. Reproduced with permission from ref. 14. Copyright 2013, Nature Publishing Group.

Chemical approach to tune the inter-layer spacing of GO laminates is generally based on controllable introducing or

removing constituents between GO sheets. Hung et al.²⁴ demonstrated that using diamine monomers to cross-link GO can effectively tune the interlayer-spacing of GO membranes from 8.7 to 10.4 Å. Compared with the intrinsic hydrogen bonds and π - π interactions in pristine GO laminates, the C-N covalent bonds formed in the cross-linked GO significantly suppressed the swelling of interlayer-spaces caused by the adsorption of water in the membranes. It benefits for the improvement of molecular sieving efficiency and long-term stability of assembled GO membranes. Also, interlayer spacing of GO laminates can be narrowed by reduction of the oxygen-containing groups on GO. In the thermal annealing process, structural alterations involved mainly hydroxyls and etheric groups while the carboxyls were much less affected. Geim and co-workers³⁹ reported that chemical reduction of GO laminates with the aid of hydroiodic or ascorbic acids can lead membranes to be highly impermeable to all gases, liquids and aggressive chemicals. Both the little structural damage during reduction and the highly decreased interlayer spacing ($d=3.6$ Å) contributes the exceptional barrier properties.

In addition, intrinsic defects are often inevitably generated in graphene-based membranes during the synthesis and transfer process of graphene-based nanosheets. Such defects are undesirable for the electrical properties of graphene-based materials⁴, however, offer potential opportunities for assembled membranes. Defects in graphene-based membranes may provide more permeation “gates” and shorter transport pathways through the stacked nanosheets, achieving higher flux¹³. Furthermore, recent studies indicated that molecular sieving property of the nanosheets can be transformed from non-selective to selective or even highly-selective if they are carefully stacked. Karnik and co-workers⁴⁰ showed that by stacking individual layers of graphene, it is possible to exponentially reduce leakage through defects in the membrane. Another study¹⁸ indicated that O₂/N₂ selectivity of PTMSP membranes deposited with few-layers CVD-grown graphene can be improved by stacking more graphene layers. An interesting work from Li et al.¹⁹ demonstrated that structural defects on GO, whose size was estimated between 0.289 and 0.33 nm, were manipulated to prepare ultrathin GO membranes, with thickness approaching 1.8 nm, by a facile filtration process. These membranes showed selectivity as high as 3400 and 900 for H₂/CO₂ and H₂/N₂ mixtures, respectively, which are 1-2 orders of magnitude higher than those of the state-of-the-art microporous membranes. Nowadays, how to precisely generate highly-selective defects in GO laminates for molecular separation is still a huge challenge.

2.4 Graphene-based composites

Generally, GO is of a layered structure with hydroxyl, carboxyl, and epoxide groups bearing on the basal plane and edge, as well as a highly dispersible derivative of graphene^{29, 31}. These favorable features enable GO with a large specific surface area and versatility through covalent or non-covalent approaches, leading to a good compatibility between GO and the host materials. Thus, integration of GO with functional materials to develop multifunctional GO-based composites have been of great interests in various fields such as water treatment, supercapacitors, biomedical engineering, photovoltaic devices, conductive polymer composites. Since inorganic-polymer composite membranes (also be referred to mixed matrix membranes) could combine the excellent processability of polymer and the unique characteristic of inorganic filler, GO-polymer composites have attracted much attention in membrane

separation^{20, 21, 41-43}. For such application, the irregular size effect of GO on the membrane structure and performance should not be ignored. Different sizes of GO can be obtained by tuning oxidation condition, controlling process of centrifugation and ultrasonic time. Moreover, a critical prerequisite to make these GO-based composite membranes is uniform dispersion of GO in aqueous or organic solution. The polar oxygen-containing functional groups of GO render it hydrophilic, making it to be exfoliated in some solvents, and dispersed particularly well in water readily achieved by sonication. In some cases, functionalization of GO would be necessary to improve the compatibility with polymer matrix, dispersion in nonaqueous medium and/or facilitating transport of target molecules.

Owing to the extraordinary water transport behavior between GO nanosheets, GO was employed as be a useful filler for pervaporation dehydration of organic-water mixtures. Gao et al.²¹ physically incorporated GO nanosheets into sodium alginate matrix to fabricate hybrid membranes. The oxygen-containing groups, structural defects, edge-to-edge slits and non-oxide regions of GO nanosheets provided channels with high selectivity and transport rate toward water molecules. They claimed that smaller nanosheet size, more structural defects and less oxygen-containing groups of GO could construct more water channels. The permselectivity of water channels were further improved by less negative charges and more non-oxide regions. In addition, the fabrication of GO-polymer composites is a promising approach to enhance the performance of proton exchange membranes. Chen and coworkers⁴¹ proposed a sulfonic acid functionalized GO/Nafion nanocomposite as proton exchange membrane which demonstrated a 4 times proton conductivity improvement over Nafion at 120 °C with 25% humidity. The result rendered graphene-based Nafion nanocomposite as a promising candidate for application in fuel cells operating at elevated temperatures. Further study indicated that functionalization of GO with hydrophilic functional groups (-NH₂, -OH, -SO₃H) not only increased the number of acid sites and consequently the water retention, but also improved the compatibility with the Nafion matrix⁴². Choi et al.⁴³ found that sulfonic acid groups functionalized GO, when being introduced into Nafion polymer, could control the state of water by means of nanoscale manipulation of the physical geometry and chemical functionality of ionic channels. The confinement of bound water within the reorganized nanochannels of GO-polymer composite membranes achieved a high proton conductivity and effective methanol rejection, leading to high-performance fuel cells.

Another great potential of GO-polymer composites lies in diverse environments for GO assembly provided by the host materials. In contrast to water for processing pristine GO membranes, polymers with various functional groups are more flexible to obtain well-defined nanostructures of GO assembly, and highly strengthen GO membrane for reliable modules and stability in practical use. Our very recent work²⁰ demonstrated that constructing hydrogen bonding between GO and polyether block amide enabled the assembly of GO nanosheets into several-layered GO stacks with molecular-sieving interlayer spacing and straight diffusion pathways (Figures 9 and 10c). With fast and selective gas transport channels, the GO laminates endowed the GO-polymer composites with excellent preferential CO₂ permeation performance (CO₂ permeability: 100 Barrer [10⁻¹⁰ cm³ (STP) cm/(cm² s cmHg)], CO₂/N₂ selectivity: 91) and extraordinary operational stability (> 6000

min), which are attractive for implementation of practical CO₂ capture. General applicability of such membranes exhibits at least two aspects: 1) facile membrane coatings on either flat or curved substrates (e.g. hollow fiber); 2) further performance improvement by increasing gas-transport channels from well-dispersed GO stacks by careful control of the polymer environment.

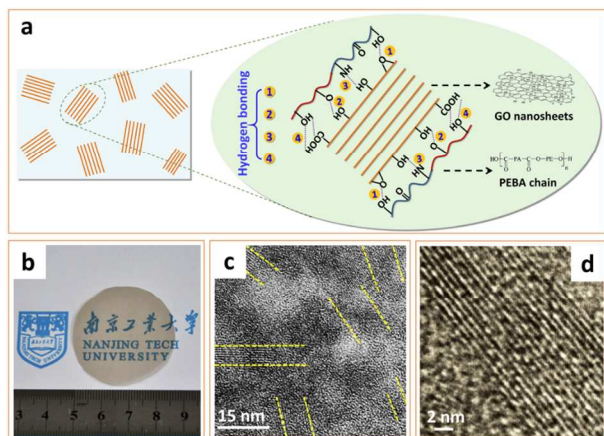


Fig. 9 (a) Schematic representation of the assembly of GO nanosheets in polymeric environment based on hydrogen bonds formed between different groups on GO and the polyether block amide (PEBA) chain, (b) digital photographs of the membrane with 0.1 wt% GO, and (c) overview (the yellow dashed lines are eye-guiding lines indicating the GO laminates in these regions) and (d) expanded TEM image of the cross section of GO-1 membrane. Reproduced with permission from ref. 20. Copyright 2015, John Wiley and Sons.

Apart from promoting molecular transport through membranes, GO nanosheets are effective nanofillers that prevent biofouling of membranes for water purification. The anti-biofouling properties of GO are mainly attributed to its oxygen-containing groups that could provide a high surface hydrophilicity and a large negative zeta potential, and inactivate bacteria. It was demonstrated that only about 1 wt% of GO nanosheets in the fabrication of nanocomposite membranes could suppress the biofouling resulted from microbial adsorption. As a result, five-fold longer time for chemical cleanings can be achieved during the wastewater treatment process⁴⁴. Moreover, having the superior adsorption capability, GO was combined with aromatic diazonium salt to form GO-NH₂ nanocomposites with a high surface area of 320 m²/g. The designed GO-NH₂ filter membrane can remove more than 98% Co(II) from the water⁴⁵. Detailed summary and discussion can be referred to recent review papers^{27, 28}. Furthermore, the intrinsic barrier properties of GO layers were employed to enhance membrane performance based on “sealing effect”. Huang et al.⁴⁶ recently combined GO with ZIFs (zeolitic imidazolate frameworks) to fabricate a bicontinuous ZIF-8@GO membrane through layer-by-layer deposition of GO on the semicontinuous ZIF-8 layer. With the aid of capillary forces and covalent bonds, the GO layer was supposed to seal the gaps between ZIF-8 crystals. Thus, the gas molecules can only permeate through the open ZIF-8 micropores (0.34 nm), leading a high molecular sieve performance for separation of H₂ (0.29 nm) from larger gas molecules. Besides, GO nanosheets can act as effective selective barriers, if they are electrostatically immobilized onto membrane surface. The function of GO nanosheets was found to reduce the surface pore diameter and narrow the pore size distribution⁴⁷ of nanofiltration membranes.

3. Applications for molecular separation

3.1 Transport mechanism

3.1.1 Inter-layer channels for molecular transport

The anomalous water transport through the Helium-leak-tight graphene-based membranes was resulted from capillary-like driving force and low-friction flow confined between 2D inter-layer channels of graphene sheets (Figure 7). By assuming that water inside these nanochannels behaves as a classical liquid, Geim and co-workers¹² employed Poiseuille’s law to describe the flow between laminar GO membranes as the following equation:

$$J = \frac{d^4 \cdot \Delta P}{12L^2 \cdot \eta \cdot h} \quad (1)$$

where d is the vertical space between adjacent graphene sheets, L the average lateral length of the graphene sheets, η the viscosity of water, and h the thickness of graphene membrane (Figure 10a). The calculation indicated that nano-confined water in GO laminates exhibited a flow enhanced by a factor of a few hundred with respect to the classical laminar regime. As we know, the basic assumptions of Hagen–Poiseuille equation are laminar flow and no-slip (or liquid flow with zero velocity) at the boundary layer. The distinct deviation of experimental flux from the classical equation suggested that the velocity of the liquid flow at graphene wall is not zero. An interfacial slip length of 10–100 nm was estimated to describe the enhanced water flow. The obtained enhancement factor and slip length were in agreement with those for sub-1-nm CNTs with single-file of moving water.

The remarkably enhanced water transport was also observed in the ultrathin chemically converted graphene nanofiltration membranes¹³ and nanostrand-channelled GO ultrafiltration membranes¹⁴ (Figure 8c). Compared with the theoretical values predicted by Poiseuille’s law, 4–6 orders of magnitude higher water flux was measured in the filtration experiments¹⁴. Han et al.¹³ found similar phenomena and explained such high flux based on the slip flow theory. The graphene (pristine) regions without functional groups possess frictionless carbon walls, which are responsible for the fast transport of water (Figure 10a). More hydrophobic liquids (isopropanol, ethanol, hexane, cyclohexane, and toluene) lead to lower flux than water, because of greater interaction between more hydrophobic liquid and graphene walls, which agreed with the slip flow theory. Nevertheless, it should be noted that the slip flow theory itself is still a controversial topic for lack of enough direct proof. Furthermore, a recent molecular simulation⁴⁸ revealed that the significant flow rate enhancement would be broken down due to a side-pinning effect by water confined between oxidized regions in GO membranes. Peng and co-workers¹⁴ demonstrated that water flow through the nanochannels between GO sheets exhibits a classic viscous feature with negligible boundary slip. In contrast with the plug-like water flow in pristine graphene, the flow profile of water exhibited a typical parabolic shape. The calculated slip length in a 3-nm GO channel is only 0.35199±0.12735 nm, more than two orders of magnitude smaller than the 48±4 nm in a 3-nm graphene channel. The resulting water flow enhancement is ~1.7, which is also much smaller than the 82±6 in a 3-nm graphene channel. The porous structures of GO laminates, including expanded interlayer gallery, wide channels formed at wrinkles, holes and inter-edge spaces, were regarded as the

main cause of fast flow of water across graphene-based membranes. Therefore, another reasonable explanation for the water flux deviated from the classical equation was proposed^{13, 14}: water molecules might go through the defects of graphene sheets (Figure 10b), leading to smaller L and higher flux calculated from Equation 1.

3.1.2 Defects or pores for molecular transport

Besides of the inter-layer channels, either intrinsic defects or drilled pores on graphene sheets can also be effectively applied for selectively transporting small molecules, as discussed in Sections 2.2 and 2.3.2. On the one side, defects or pores could provide diffusion shortcuts for molecules going through the graphene-based membranes (Figure 10b). On the other side, the defects or pores would exhibit molecular sieving properties if elaborate stacking^{18, 19} or precise drilling^{10, 11} of graphene or GO nanosheets is carried out. It was claimed that, in ultrathin molecular-sieving GO membranes for selective hydrogen separation, the major transport pathway is selective structural defects within GO nanosheets rather than the inter-layer spacing¹⁹. Such speculation was supported by the following observation: with narrowing interlayer spacing of GO membranes by reduction, water permeance was decreased approximately three orders of magnitude, but no obvious gas permeance change was found.

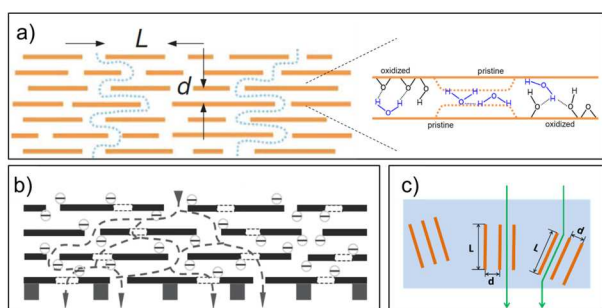


Fig. 10 Molecular transport through (a) inter-layer channels of GO laminates. Reproduced with permission from ref. 12. Copyright 2012, the American Association for the Advancement of Science; (b) inter-layer channels of GO laminates and holes on graphene sheets. Reproduced with permission from ref. 13. Copyright 2013, John Wiley and Sons; (c) inter-layer channels of random-stacked GO laminates incorporated in polymer matrix. Reproduced with permission from ref. 20. Copyright 2015, John Wiley and Sons. L : length of the GO nanosheets, d : d-spacing of GO laminates.

The atmospheric pressure effusion through atomically thin pores in graphene bilayer revealed distinct effusive, transition and collective flow regimes¹⁰. It was found that the relationship between pore size and gas permeance can be characterized by two theories: free molecular transport (effusion) for small-size pores and modified Sampson's model for large-size pores. Generally, effusive flow through membrane is desirable for separating gas mixtures, which can be explained by Knudsen transport of gases in nanoporous membranes as follows:

$$J = \frac{\Delta P}{\sqrt{2\pi m k_B T}} \quad (2)$$

where J is gas permeance, P the pressure, m the molecular weight, k_B the Boltzmann constant, T the temperature. According to Equation 2, gas transport is determined by the pore size of the graphene membrane and the free path length of the molecules in a gas mixture. Knudsen diffusion leads to separation of gases with large differences in their molecular

weights. As predicted, porous graphene bilayer with smallest pores (7.6 nm) showed the highest selectivity, which is close to the theoretical maximum predicted by the effusion theory for H_2/CO_2 selectivity of 4.69. And the membrane selectivity had a clear decay as the pore size of graphene layer increased, resulting from the increased role of collective flow. Additionally, the influence of pore size on water transport through nanoporous graphene membrane was also studied by molecular dynamics simulations⁴⁹. It was indicated that as the membrane pore is larger than 2.75 nm, water flux was higher through the graphene membrane, compared to that of the CNT membrane. This is due to the absence of single-file structure and more bulk-like water neighbors and reduced permeation energy barrier at the entrance.

3.1.3 Functional groups for facilitating molecular transport

In addition to inter-layer channels and pores or defects of graphene layers, the functional groups on graphene-derived materials (e.g., GO), play another important role in determining molecular transport through graphene-based membranes, as well. Adding functional groups into the graphene layer offers great potential in constructing molecular interactions between species and membrane, which may facilitate transporting some of the molecules. First, the oxygen-containing groups on the basal plane and edge of GO, would interact with water molecules to form hydrogen bonds, prohibiting the fast water transport through GO membrane channels⁴⁸. In contrast, owing to the hydrophilic nature, these hydroxyl, carboxyl, and epoxide groups are able to selectively adsorb water molecules from solvent-water mixtures, enhancing the pervaporation performance of GO membranes for solvent dehydration. We observed that water-selective GO membrane had a much higher water sorption ability than organic compounds (methanol, dimethyl carbonate), according to quartz crystal microbalance measurement¹⁶. Moreover, the polar groups such as $-COOH$, $-OH$ on GO could form favorable interactions with the polar individual C–O bonds on CO_2 , providing a preferential site for CO_2 adsorption. Adsorption test indicated that the gas adsorption of GO powders followed the order of $CO_2 > CH_4 > N_2 > H_2$ ¹⁹. The preferential adsorption is able to either retard or promote CO_2 transport, relying on the microstructures of GO-based membranes. For instance, although showing CO_2 -philic adsorption behavior, few-layered GO membranes prepared by different stacking methods (Figure 5b) exhibited either nanoporous (method 1) or molecular-sieving (method 2) characteristics, leading to H_2 -selective (H_2/CO_2 selectivity = 30) or CO_2 -selective permeation membranes (CO_2/N_2 selectivity = 20), respectively¹⁸.

Second, the presence of negatively charged groups on GO nanosheets could afford electrostatic interaction with the charged molecules or ions in nanofiltration and salt rejection process^{22, 35}. According to exclusion theory, the potential at the interphase of solution and membrane tends to exclude co-ions from the membrane. In order to keep the electro-neutrality of the solution on each side of the membrane, the counter ions are rejected as well¹³. Based on ion penetration tests and molecular calculations, Zhu and co-workers⁵⁰ proposed that the competition between cation- π interactions of the cations considered with the sp^2 clusters within GO nanocapillaries and desolvation effect of ions determines selective ions diffusion through laminar GO membranes. Such phenomenon is similar to some ion transport processes across cellular membranes involving the interactions between cations and aromatic side chains of the hydrophobic amino acids.

Practically, the molecular transport through graphene-based membranes might be governed by synergy effects of the above two or three factors (i.e., inter-layer channels, holes/defects and functional groups). The stacked GO layers decorated by selective-defects and oxygen-containing groups provide not only fast and selective nanochannels but also preferential interactions sites for transporting molecules or ions. As laminar GO membrane was applied for dehydration of solvent/water mixtures, water molecules were preferentially adsorbed onto the oxygen-containing functional groups around GO and then penetrated into the inter-layer channels and diffused rapidly due to their low friction contact with the hydrophobic central region²⁴. Moreover, the inter-layer space can be enlarged by introducing water into the dry GO layer when immersing GO laminates into aqueous solution. While the immersion in solvents such as alcohols had little effect on the d-spacing of GO membranes. As for GO nanofiltration membranes, it was claimed that the spacing between GO layers and the charges on GO nanosheets are two dominant factors determining the rejection performance²² (Figure 10b). Furthermore, the transport mechanism for membranes derived from graphene-based composites would be more complicated. Because it is also determined by dispersion status of graphene nanosheets and chemical nature of matrix. With regard to the GO-polymer hybrid membranes, the polymer matrix would enable the assembly of GO nanosheets into GO stacks in random directions. In addition to the tortuous pathways through parallel-stacked GO nanosheets, there are more straight and upright pathways provided by the inclined and even vertical GO stacks (Figure 10c)²⁰. The vertical GO stacks have a very short transport distance (it equals L), which is 2-3 orders of magnitude (h/d) shorter than that of the parallel stacks. In view of this, the accomplishment of vertical array of GO stacks as pristine membrane or embeded in polymer matrix will be able to achieve highly-improved separation permeance.

3.2 Separation performance

3.2.1 Pressure filtration

The exciting finding of unimpeded water permeation through GO laminates encouraged people to investigate graphene-based membranes for water purification, which is often operated by pressure filtrations. Table 1 summarized the separation performance. The simulated porous graphene monolayer with around 2-nm hydrogenated or hydroxylated pores has been predicted to be able to effectively filter NaCl salt from water with ultra-high flux⁷. Nevertheless, the fabrication and usage of such ideal nanoporous graphene membranes remains a big technical challenge. In contrast, laminar GO membranes readily prepared by vacuum filtration or layer-by-layer methods have been experimentally studied regarding the filtration processes of nanofiltration (NF), ultrafiltration (UF) and forward osmosis (FO). In order to obtain applicable permeate flux and mechanical strength, sub-micrometer or few-micrometers thick GO laminates were deposited on top of porous polymeric substrates such as polycarbonate (PC), polyvinylidene fluoride (PVDF), polysulfone (PSF) and poly(acrylonitrile) (PAN).

The water purification performance of the GO membranes was evaluated in two main aspects: retention of organic dyes and salts rejection. Generally, the GO membranes were proven to be efficient for rejecting organic dyes such as direct yellow (DY), Evans blue (EB) and methylene blue (MB) with the rejection of more than 85%. However, the rejections of laminar GO membranes for monovalent or divalent salts were relatively

low (<50%). This is because the inter-layer spaces between GO layers are estimated as 1-5 nm, which is within the molecular size of organic dyes while too large for retaining salts. The water flux is increased with enlarging the inter-layer space of the GO laminates. Furthermore, creating more porous structure and reducing channel length would be effective approaches for flow enhancement in GO membranes, achieving much higher water flux than the commercial membranes with comparative rejection¹⁴. However, there is still a gap between the prepared porous single-layer graphene or GO laminates and simulated nanoporous graphene, regarding to the filtration pressure, water flux and rejection. The implementation of graphene-based membranes for water desalination via reverse osmosis (RO) process would be realized if further narrowing the pore size and/or improving pore density in large-scale, as well as strengthening the mechanical properties.

3.2.2 Pervaporation

Pervaporation is a membrane process that could realize molecular separation for liquid mixtures. A feed solution is passed over pervaporation membrane surface and some of the components are able to preferentially pass through the membrane and concentrated as vapors in the permeate. The anomalous water transport between graphene layers and the intrinsic hydrophilicity of GO nanosheets promise GO-based membranes great opportunities in pervaporation dehydration of solvent. Until now most of them were applied for selective removing water from aqueous solution containing concentrated alcohol such as ethanol (EtOH), isopropyl alcohol (IPA) and *n*-butanol (1-BtOH). As listed in Table 2, these laminar GO membranes were fabricated by depositing GO nanosheets on the surface of porous substrates via pressure-driven or vacuum filtration method. The thickness of most GO laminates was generally controlled at sub-micrometer size in order to facilitate a low transport resistance through the membrane. Since molecular sizes of the solvents are much smaller than the organic dyes, which is often less than 1 nm, the inter-layer spaces of the GO laminates should be much smaller than that for NF. According to the XRD analysis, the d-spacing of laminar GO membranes used for effective pervaporation dehydration was about 0.8-0.9 nm.

The “empty” space within the GO layers can be considered as interlayer d-spacing subtracting the graphene thickness (0.35 nm) and the space occupied by the oxygen-containing functional groups of GO (0.2 nm)²⁴. With the given d-spacing of 0.85-0.93 nm in Table 2, the “empty” space is estimated as 0.30-0.38 nm. This space is between the kinetic diameters of water and alcohols, allowing water to pass through but blocking alcohols. Laminar GO membranes exhibited a high flux and good separation factor for alcohols dehydration, compared with the reported polymeric membranes. Membrane selectivity was further improved by cross-linking GO layers with small molecules such as ethylenediamine (EDA), as a result of tuning the inter-layer space and hydrophilicity. Meanwhile, the cross-linked GO laminates showed a good stability in a long-term operation of 90 wt% ethanol/water dehydration for 120 h at 30 °C.

3.2.3 Gas separation

Graphene is an excellent starting point for developing gas separation membranes because of its atomic thickness, high mechanical strength, relative inertness and impermeability to all standard gases. Porous graphene layer, graphene laminates and graphene-based composites were all used for purifying

Table 1 Graphene-based membranes for pressure filtration

Graphene-based membranes	Preparation method	Membrane structure ^a	Feed system	Membrane process	Water flux (L/m ² /h/bar)	Rejection	Ref.
Porous graphene monolayer	H- pore OH-pore (Simulation)	$d = 2.3$ nm $d = 1.6$ nm	72 g/L NaCl	RO ~100 MPa	1625 2750	~100% ~100%	7
Porous graphene monolayer	oxygen plasma etching	$d = 0.5-1$ nm	1 M KCl	Osmosis ~5 MPa	250	~100%	23
Wet GO/PC	Vacuum filtration	Not available	0.01 mM DY	UF 0.1 MPa	45	67%	38
GO/PC	Vacuum filtration	$l = 1.9$ μ m	15 mM EB	UF 0.1MPa	71	85%	14
Nanostrand channeled GO/PC	Vacuum filtration	$d = 3-5$ nm $l = 2$ μ m	15 mM EB	UF 0.1MPa	695	83.5%	14
Base-refluxing reduced GO/PVDF	Vacuum filtration	$d = 1-2$ nm $l = 22$ nm	0.02 mM MB	NF 0.1 MPa	21.8	99.2%	13
Base-refluxing reduced GO/PVDF	Vacuum filtration	$l = 53$ nm	20 mM Na ₂ SO ₄ 20 mM NaCl 7.5 mg/L MB	NF 0.5 MPa	3.3	20% 40% 46-66%	13
TMC cross-linked GO/PSF	Layer-by-layer	$d = 1$ nm	20 mM Na ₂ SO ₄ 20 mM NaCl	NF 0.34 MPa	8-27.6	6-19% 26-46%	15
PAH cross-linked GO/PAN	Layer-by-layer	$d = 1$ nm	1 M sucrose	FO 0.34 MPa	2.1-5.8	~99%	15
GO-PEI composite/ PAI hollow fiber	Electrostatically dip-coating	$l = 1$ μ m	500 ppm MaCl ₂	NF 0.1 MPa	11	85%	47

^a d : pore size; l : membrane thickness; PAI: poly(amide-imide); PEI: polyethyleneimine; TMC: 1,3,5-benzenetricarbonyl trichloride; PAH: poly(allylaminehydrochloride).

Table 2 Graphene-based membranes for pervaporation

Graphene-based membranes	Preparation method	Membrane structure ^a	Feed condition	Total flux (g m ⁻² h ⁻¹)	Separation factor	Ref.
EDA-crosslinked GO/CA	Pressure-assisted self-assembly	$ds = 0.93$ nm $l = 412$ nm	80 °C, 90 wt% EtOH-water	2297	4491	24
GO/mPAN	Pressure-assisted self-assembly	$ds = 0.85$ nm $l = 231$ nm	70 °C, 70 wt% IPA-water 70 °C, 90 wt% 1-BtOH-water	4137 4340	1164 1791	16 34
GO/ceramic hollow fiber	Vacuum suction	$l = 1$ μ m	25 °C, 97.4 wt% DMC/water	1702	743	17
Freestanding GO laminate	Pressurized ultrafiltration	$l = 2$ μ m	24 °C, 75 wt% EtOH-water	1300	211	24
GO-sodium alginate composite	Film casting	$l = 1.6$ μ m	76 °C, 90 wt% EtOH-water	1699	1566	21

^a ds : d -spacing; l : membrane thickness; CA: cellulose acetate; mPAN: modified PAN: polyacrylonitrile; DMC: dimethyl carbonate

hydrogen or carbon dioxide from gas mixtures, and for oxygen/nitrogen separation in some case.

Molecular simulations⁹ demonstrated that extremely high selectivity on the order of 10²³ for H₂/CH₄ can be achieved in the graphene monolayer with a 2.5 Å all-hydrogen passivated pore. The experimental drilling Angstrom scale pores in micrometer-sized bilayer graphene sheet, however, obtained much lower selectivity compared with the simulation value³², as discussed in Section 2.2. In view of real application, high-density pores and large-area membranes are urgently needed for porous graphene membranes. A stimulating attempt has realized the separation of gas mixtures through porous graphene bilayer under cross flow conditions¹⁰. Since the drilled pore size can only be as small as 7.6 nm, the porous graphene membrane showed Knudsen diffusion selectivity for H₂/CO₂ but orders of magnitude superior gas permeance than the reported values.

The development of laminar graphene membranes provides a feasible approach to push graphene-based membranes into practical gas separation, including ultra-thin membranes with few graphene layers prepared by chemical

vapor deposition or GO layers fabricated by spinning coating and vacuum filtration methods. In particular, either small molecule (e.g., H₂^{9, 18, 19, 32, 37, 46}) or large molecule (e.g., CO₂^{18, 20}) would preferentially go through the few-layered GO membranes with different microstructures. The present of intrinsic or post-treated selective defects was in favor of enhancing the molecular sieving properties of laminar GO membranes. In addition, GO nanosheets were acted as an additive to incorporate into polymer to form GO-based composite membranes²⁰. Thus, the permeability and selectivity of the polymeric membrane were simultaneously improved owing to the fast and selective channels provided by GO laminates. In contrast, the layer-by-layer deposition of impermeable GO layers between ZIF-8 crystals reduced nonselective transport pathway through intercrystalline defects, and the rigid GO layer around the ZIF-8 crystals can constrict lattice flexibility of ZIF-8. So the GO deposition markedly enhanced the molecular sieving selectivity of ZIF-8 membranes⁴⁶.

Table 3 Graphene-based membranes for gas separation

Graphene-based membranes	Preparation method	Membrane structure ^a	Feed condition ^b	Permeate rate /permeance/ permeability ^c	Selectivity	Ref.
Porous graphene monolayer	Simulation All-H passivation	$d = 2.5 \text{ \AA}$	H ₂ /CH ₄	$1 \times 10^{-20} \text{ mol s}^{-1} \text{ Pa}^{-1}$	10 ²³	9
Porous graphene bilayer	Ultraviolet-induced oxidative etching	$d = 3.4 \text{ \AA}$	H ₂ /CH ₄	$4.5 \times 10^{-23} \text{ mol s}^{-1} \text{ Pa}^{-1}$	10 ⁴	32
Porous graphene bilayer	Focused ion beam perforation	$d = 7.6 \text{ nm}$	H ₂ /CO ₂	$5.0 \times 10^{-3} \text{ mol m}^{-2} \text{ s}^{-1} \text{ Pa}^{-1}$	4.6	38
Few-layered graphene/PTMSP	Chemical vapor deposition	$l = 5$ graphene layers	O ₂ /N ₂	29 Barrer	6	18
Few-layered GO/PES	Spinning coating Thermal reduced	$l = 3\text{-}7 \text{ nm}$	CO ₂ /N ₂	100 GPU	20	18
		Not available	H ₂ /CO ₂ (140 °C)	1000 GPU	40	
GO/AAO	Vacuum filtration	$l = 9 \text{ nm}$	H ₂ /CO ₂ H ₂ /N ₂	$10^{-7} \text{ mol m}^{-2} \text{ s}^{-1} \text{ Pa}^{-1}$	3400 900	19
GO-PEBA composite	Film casting	$l = 5 \text{ }\mu\text{m}$	CO ₂ /N ₂	100 Barrer	91	20
			H ₂ /CO ₂		15	
ZIF-8@GO composite	Layer-by-layer	$l = 100 \text{ nm}$ for GO layer	H ₂ /N ₂	$10^{-7} \text{ mol m}^{-2} \text{ s}^{-1} \text{ Pa}^{-1}$	91	46
			H ₂ /CH ₄		139	
			H ₂ /C ₃ H ₈ (250 °C)		3817	

^a d : pore size; l : membrane thickness; ^b operated at room temperature unless otherwise indicated. ^c 1 GPU = $10^{-6} \text{ cm}^3 \text{ (STP)/(cm}^2 \text{ s cmHg)}$; 1 Barrer = $10^{-10} \text{ cm}^3 \text{ (STP) cm/(cm}^2 \text{ s cmHg)}$. PTMSP: poly(1-methylsilyl-1-propyne); PES: polyether sulfone; AAO: anodic aluminum oxide.

4. Conclusions and perspectives

In summary, a large number of investigations in recent a few years demonstrated that graphene-based membranes showed extraordinary permeation properties, opening the door to ultra-fast and highly-selective transport of water, gases and some specific small molecules. The unique one-atom-thick structure and excellent stiffness promised nanoporous graphene layers as precise molecular sieves. Nevertheless, facile and large-area perforation of graphene remains a technical challenge. With oxygen-containing groups and mass-produced characters, GO nanosheets could be readily assembled into laminates or incorporated with polymers or inorganics as composites. The resulted GO-based membranes have exhibited extraordinary water flow enhancement for water purification and excellent gas separation properties that transcend the performance limitation of conventional membranes. With deep insights into transport mechanisms, the inter-layer channels, selective holes/defects and functional groups of graphene-based membranes are considered as three crucial factors governing the molecular transport behavior.

Despite great progresses have been achieved, there are still several emerging challenges and opportunities for both the scientific community and engineers, and some of them are highlighted as follows. (1) *Membrane materials*: as the starting point for developing membranes, graphene-based materials demand for more smart physical or chemical routes to produce them with leak-free, large-area and cost-effective qualities. Further study is also needed to control the size, functional groups and charged properties of graphene and its derivatives in order to finely tune the membrane microstructures and chemistries. (2) *Membrane fabrication*: the established approaches of processing graphene or GO into membranes are not delicate enough compared with state-of-the-art membranes. Much effort should be taken to precisely control the pore size or inter-layer space, especially to realize sub-nanometer channels within graphene-based membranes. Highly inter-locked stacking, molecular intercalation, pore functionalization or reduction treatment might be helpful to accomplish this purpose. Moreover, manipulating the flow direction and

distance across the GO laminates or composites is expected to further advance the membrane separation performance. The achievement of vertically oriented inter-layer channels will allow ultra-fast permeation through graphene-based membranes. (3) *Separation mechanism*: the relationship between the anomalous transport mechanism in graphene-based membranes and classic transport theory remains elusive. More specific and accurate transport models should be proposed for graphene-based membranes by considering the unique 2D frictionless nanochannels between graphene layers. The study of confined mass transfer in the sub-nanometer sized space deserves particular attention. Advanced characterization techniques combined with simulation tools can be employed to better understand the respective effect of inter-layer spaces, selective defects and functional groups on transport behavior. (4) *Membrane application*: various exciting yet challenging applications of graphene-based membranes in desalination, battery separator and hydrophobic pervaporation are a very worthy of being explored upon creating selective passages with tunable size and functionality. Several specific issues need to be addressed toward the implementation of graphene-based membranes for separation such as the stability of laminar membranes in cross-flow conditions, reliable modules for ultra-thin few-layered membranes. Finally, we anticipate that the fundamental understanding and technical processing related to graphene-based membranes will throw light on the rapid growing interest in membranes and functional films derived from 2D materials.

Acknowledgements

We acknowledge the National Natural Science Foundation of China (Nos. 21406107, 2149580015, 21476107), Innovative Research Team Program by the Ministry of Education of China (No. IRT13070), Natural Science Foundation of Jiangsu Province (No. BK20140930) and the Project of Priority Academic Program Development of Jiangsu Higher Education Institutions (PAPD) for financial support.

Notes and references

State Key Laboratory of Materials-Oriented Chemical Engineering, College of Chemistry and Chemical Engineering, Nanjing Tech University (former Nanjing University of Technology), 5 Xinmofan Road, Nanjing 210009, PR China. E-mail: wqjin@njtech.edu.cn (Prof. W.Q. Jin); Tel.: +86 25 83172266

1. D. L. Gin and R. D. Noble, *Science*, 2011, 332, 674-676.
2. A. K. Geim and K. S. Novoselov, *Nat Mater*, 2007, 6, 183-191.
3. B. Mi, *Science*, 2014, 343, 740-742.
4. A. K. Geim, *Science*, 2009, 324, 1530-1534.
5. J. S. Bunch, S. S. Verbridge, J. S. Alden, A. M. van der Zande, J. M. Parpia, H. G. Craighead and P. L. McEuen, *Nano Letters*, 2008, 8, 2458-2462.
6. V. Berry, *Carbon*, 2013, 62, 1-10.
7. D. Cohen-Tanugi and J. C. Grossman, *Nano Letters*, 2012, 12, 3602-3608.
8. K. Sint, B. Wang and P. Král, *Journal of the American Chemical Society*, 2008, 130, 16448-16449.
9. D.-e. Jiang, V. R. Cooper and S. Dai, *Nano Letters*, 2009, 9, 4019-4024.
10. K. Celebi, J. Buchheim, R. M. Wyss, A. Droudian, P. Gasser, I. Shorubalko, J.-I. Kye, C. Lee and H. G. Park, *Science*, 2014, 344, 289-292.
11. S. C. O'Hern, M. S. H. Boutilier, J.-C. Idrobo, Y. Song, J. Kong, T. Laoui, M. Atieh and R. Karnik, *Nano Letters*, 2014, 14, 1234-1241.
12. R. R. Nair, H. A. Wu, P. N. Jayaram, I. V. Grigorieva and A. K. Geim, *Science*, 2012, 335, 442-444.
13. Y. Han, Z. Xu and C. Gao, *Advanced Functional Materials*, 2013, 23, 3693-3700.
14. H. Huang, Z. Song, N. Wei, L. Shi, Y. Mao, Y. Ying, L. Sun, Z. Xu and X. Peng, *Nat Commun*, 2013, 4.
15. M. Hu and B. Mi, *Journal of Membrane Science*, 2014, 469, 80-87.
16. W.-S. Hung, Q.-F. An, M. De Guzman, H.-Y. Lin, S.-H. Huang, W.-R. Liu, C.-C. Hu, K.-R. Lee and J.-Y. Lai, *Carbon*, 2014, 68, 670-677.
17. K. Huang, G. Liu, Y. Lou, Z. Dong, J. Shen and W. Jin, *Angewandte Chemie International Edition*, 2014, 53, 6929-6932.
18. H. W. Kim, H. W. Yoon, S.-M. Yoon, B. M. Yoo, B. K. Ahn, Y. H. Cho, H. J. Shin, H. Yang, U. Paik, S. Kwon, J.-Y. Choi and H. B. Park, *Science*, 2013, 342, 91-95.
19. H. Li, Z. Song, X. Zhang, Y. Huang, S. Li, Y. Mao, H. J. Ploehn, Y. Bao and M. Yu, *Science*, 2013, 342, 95-98.
20. J. Shen, G. Liu, K. Huang, W. Jin, K.-R. Lee and N. Xu, *Angewandte Chemie International Edition*, 2015, 54, 578-582.
21. K. Cao, Z. Jiang, J. Zhao, C. Zhao, C. Gao, F. Pan, B. Wang, X. Cao and J. Yang, *Journal of Membrane Science*, 2014, 469, 272-283.
22. M. Hu and B. Mi, *Environmental Science & Technology*, 2013, 47, 3715-3723.
23. S. P. Surwade, S. N. Smirnov, I. V. Vlassioux, R. R. Unocic, G. M. Veith, S. Dai and S. M. Mahurin, *Nat Nano*, 2015, doi:10.1038/nnano.2015.37.
24. W.-S. Hung, C.-H. Tsou, M. De Guzman, Q.-F. An, Y.-L. Liu, Y.-M. Zhang, C.-C. Hu, K.-R. Lee and J.-Y. Lai, *Chemistry of Materials*, 2014, 26, 2983-2990.
25. Y. P. Tang, D. R. Paul and T. S. Chung, *Journal of Membrane Science*, 2014, 458, 199-208.
26. H. Huang, Y. Ying and X. Peng, *Journal of Materials Chemistry A*, 2014, 2, 13772-13782.
27. K. A. Mahmoud, B. Mansoor, A. Mansour and M. Khraisheh, *Desalination*, 2015, 356, 208-225.
28. P. S. Goh and A. F. Ismail, *Desalination*, 2015, 356, 115-128.
29. D. R. Dreyer, S. Park, C. W. Bielawski and R. S. Ruoff, *Chemical Society Reviews*, 2010, 39, 228-240.
30. D. A. Dikin, S. Stankovich, E. J. Zimney, R. D. Piner, G. H. B. Dommett, G. Evmenenko, S. T. Nguyen and R. S. Ruoff, *Nature*, 2007, 448, 457-460.
31. O. C. Compton and S. T. Nguyen, *Small*, 2010, 6, 711-723.
32. S. P. Koenig, L. Wang, J. Pellegrino and J. S. Bunch, *Nat Nano*, 2012, 7, 728-732.
33. Z. P. Smith and B. D. Freeman, *Angewandte Chemie International Edition*, 2014, 53, 10286-10288.
34. C.-H. Tsou, Q.-F. An, S.-C. Lo, M. De Guzman, W.-S. Hung, C.-C. Hu, K.-R. Lee and J.-Y. Lai, *Journal of Membrane Science*, 2015, 477, 93-100.
35. P. Sun, M. Zhu, K. Wang, M. Zhong, J. Wei, D. Wu, Z. Xu and H. Zhu, *ACS Nano*, 2013, 7, 428-437.
36. Y. Lou, G. Liu, S. Liu, J. Shen and W. Jin, *Applied Surface Science*, 2014, 307, 631-637.
37. R. K. Joshi, P. Carbone, F. C. Wang, V. G. Kravets, Y. Su, I. V. Grigorieva, H. A. Wu, A. K. Geim and R. R. Nair, *Science*, 2014, 343, 752-754.
38. L. Qiu, X. Zhang, W. Yang, Y. Wang, G. P. Simon and D. Li, *Chemical Communications*, 2011, 47, 5810-5812.
39. Y. Su, V. G. Kravets, S. L. Wong, J. Waters, A. K. Geim and R. R. Nair, *Nat Commun*, 2014, 5.
40. M. S. H. Boutilier, C. Sun, S. C. O'Hern, H. Au, N. G. Hadjiconstantinou and R. Karnik, *ACS Nano*, 2014, 8, 841-849.
41. H. Zarrin, D. Higgins, Y. Jun, Z. Chen and M. Fowler, *The Journal of Physical Chemistry C*, 2011, 115, 20774-20781.
42. A. Enotiadis, K. Angieli, N. Baldino, I. Nicotera and D. Gournis, *Small*, 2012, 8, 3338-3349.
43. B. G. Choi, J. Hong, Y. C. Park, D. H. Jung, W. H. Hong, P. T. Hammond and H. Park, *ACS Nano*, 2011, 5, 5167-5174.
44. J. Lee, H.-R. Chae, Y. J. Won, K. Lee, C.-H. Lee, H. H. Lee, I.-C. Kim and J.-m. Lee, *Journal of Membrane Science*, 2013, 448, 223-230.
45. F. Fang, L. Kong, J. Huang, S. Wu, K. Zhang, X. Wang, B. Sun, Z. Jin, J. Wang, X.-J. Huang and J. Liu, *Journal of Hazardous Materials*, 2014, 270, 1-10.
46. A. Huang, Q. Liu, N. Wang, Y. Zhu and J. Caro, *Journal of the American Chemical Society*, 2014, 136, 14686-14689.
47. K. Goh, L. Setiawan, L. Wei, R. Si, A. G. Fane, R. Wang and Y. Chen, *Journal of Membrane Science*, 2015, 474, 244-253.
48. N. Wei, X. Peng and Z. Xu, *ACS Applied Materials & Interfaces*, 2014, 6, 5877-5883.
49. M. E. Suk and N. R. Aluru, *The Journal of Physical Chemistry Letters*, 2010, 1, 1590-1594.
50. P. Sun, F. Zheng, M. Zhu, Z. Song, K. Wang, M. Zhong, D. Wu, R. B. Little, Z. Xu and H. Zhu, *ACS Nano*, 2014, 8, 850-859.